JOURNAL OF VIROLOGY, Apr. 1992, p. 2443–2455
0022-538X/92/042443-13$02.00/0

Vol. 66, No. 4

Studies on the Fusion Peptide of a Paramyxovirus Fusion Glycoprotein: Roles of Conserved Residues in Cell Fusion

CURT M. HORVATH[1] AND ROBERT A. LAMB[1,2]*

Department of Biochemistry, Molecular Biology and Cell Biology[1] and Howard Hughes Medical Institute,[2] Northwestern University, Evanston, Illinois 60208-3500

Received 10 December 1991/Accepted 17 January 1992

The role of residues in the conserved hydrophobic N-terminal fusion peptide of the paramyxovirus fusion (F) protein in causing cell-cell fusion was examined. Mutations were introduced into the cDNA encoding the simian virus 5 (SV5) F protein, the altered F proteins were expressed by using an eukaryotic vector, and their ability to mediate syncytium formation was determined. The mutant F proteins contained both single- and multiple-amino-acid substitutions, and they exhibited a variety of intracellular transport properties and fusion phenotypes. The data indicate that many substitutions in the conserved amino acids of the simian virus 5 F fusion peptide can be tolerated without loss of biological activity. Mutant F proteins which were not transported to the cell surface did not cause cell-cell fusion, but all of the mutants which were transported to the cell surface were fusion competent, exhibiting fusion properties similar to or better than those of the wild-type F protein. Mutant F proteins containing glycine-to-alanine substitutions had altered intracellular transport characteristics, yet they exhibited a great increase in fusion activity. The potential structural implications of this substitution and the possible importance of these glycine residues in maintaining appropriate levels of fusion activity are discussed.

Penetration of enveloped viruses into a host cell occurs by means of direct fusion of the viral envelope with cellular membranes, resulting in delivery of the viral genome (in the form of a capsid or nucleocapsid) into the cytoplasm of the target cell. A large body of data for viruses such as orthomyxoviruses, togaviruses, rhabdoviruses, bunyaviruses, and some retroviruses indicates that, following attachment of the virus to a cell surface receptor, the viruses are endocytosed and transported to a low-pH endosomal compartment where the low pH triggers the fusion of the viral envelope with the cellular plasma membrane, releasing the viral genome into the cytoplasm. For other viruses, such as paramyxoviruses, herpesviruses, coronaviruses, and human immunodeficiency virus, the majority of the available evidence indicates that the viral envelope fuses directly with the cellular plasma membrane, releasing the viral genome into the cytoplasm. In all cases, fusion of the viral envelope with a cellular membrane is mediated by a viral envelope glycoprotein (reviewed in references 58, 66, and 67). An important consequence of virus-induced fusion at neutral pH is cell-to-cell fusion causing the intercellular spread of virus, the formation of syncytia, and subsequent cell death.

The fusion (F) glycoprotein of paramyxoviruses is a type I integral membrane protein that has been shown to be involved in virus penetration, hemolysis, and cell fusion (16, 52). The F protein is synthesized as an inactive precursor (F_0) that is cleaved by a host cell proteolytic enzyme to form the biologically active protein consisting of the disulfide-linked chains F_1 and F_2, resulting in the release of the new N terminus of F_1 (52–54). Detergent binding and spectroscopic studies indicate that cleavage of F_0 causes a conformational change in the molecule, resulting in the exposure of previously solvent-inaccessible hydrophobic domains, and that there is a concomitant increase in the α-helical nature of the protein (20). Both protein sequencing studies of the F protein and nucleotide sequencing studies of the cDNA of the F protein genes of many paramyxoviruses indicate that the N-terminal 20 residues of F_1 are extensively hydrophobic and this region of the F protein is highly conserved among paramyxovirus F proteins (up to 90% identity; see Fig. 1A) (54; reviewed in reference 31). This led to the suggestion that the N-terminal region of F_1 (fusion peptide) is directly involved in promoting fusion with the target membrane (13, 46, 54). Evidence in support of this notion includes the finding that synthetic peptides that mimic the fusion peptide sequence inhibit both cell fusion and virus penetration (45, 46). In addition, the fusion peptide is sufficiently hydrophobic to act as an anchor (stop-transfer domain) of a heterologous membrane protein (39), indicating that the fusion peptide can form stable interactions with membranes. Other evidence that the fusion peptide can interact with target lipid bilayers was obtained by labeling it with photoactive lipid probes (2, 34).

It has been shown previously that the paramyxovirus simian virus 5 (SV5) F gene cDNA (37), when expressed in CV-1 cells by using SV40 recombinant viruses, is biologically active, causing syncytium formation (38, 41). Thus, this provides an assay system in which the contribution of residues in the fusion peptide to syncytium formation can be tested. The invariant nature of many of the residues of the fusion peptide between paramyxovirus F proteins suggests a role more complex than preservation of hydrophobic residues required for a membrane-intercalating domain: neither signal sequences nor membrane anchorage domains show sequence conservation beyond their hydrophobic nature (64). It has been noted that if the fusion peptide is assumed to be an α-helix, then the invariant residues are located on one face of the helix (Fig. 1B) (55). The significance of this is unknown, but it is of interest that membrane spanning domains of proteins are usually thought to be α-helical regions based on theoretical predictions and also

* Corresponding author.

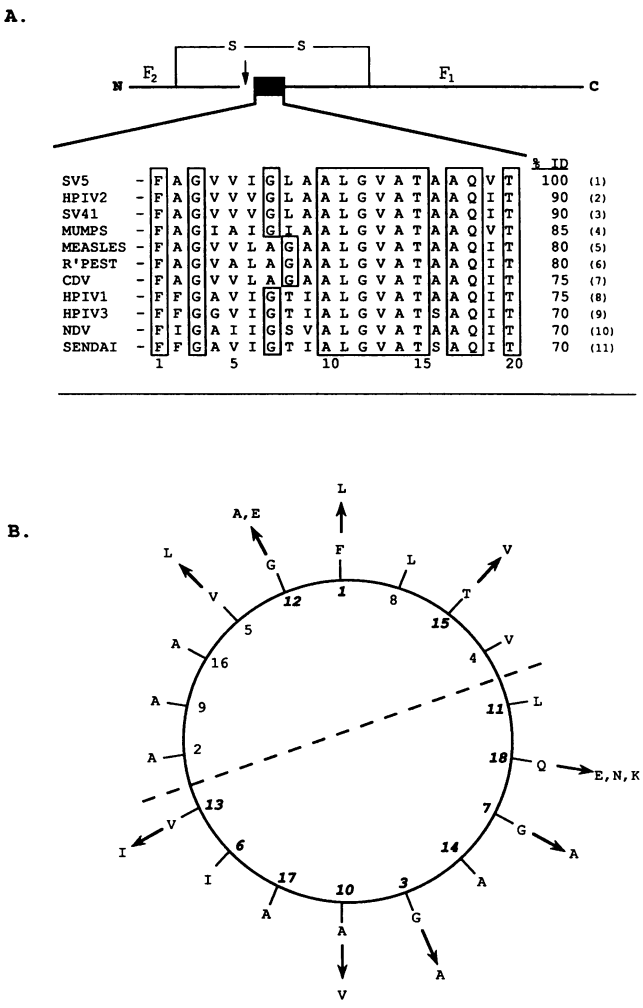

FIG. 1. (A) Schematic diagram of the SV5 F protein fusion peptide domain and its amino acid sequence conservation between paramyxoviruses. The line represents the disulfide-linked F protein subunits F_1 and F_2; the arrow indicates the cleavage site. The shaded box represents the F_1 N-terminal fusion peptide. The expanded section shows a comparison of the amino acid sequence of the fusion peptides of SV5 and 10 other paramyxovirus fusion proteins, with the boxed regions indicating amino acid identity. %ID = percentage identity to the SV5 sequence in the N-terminal 20 amino acids. Lines show data from the following references: 1, 37; 2, 22; 3, 62; 4, 65; 5, 44; 6, 61; 7, 63; 8, 28; 9, 57; 10, 27; 11, 19. (B) Helical wheel representation of the SV5 F_1 fusion peptide showing residues changed by mutagenesis. The amino acids of the F_1 amino terminus are numbered; italics indicate the invariant amino acid residues. Point mutations constructed and described in this work are shown by arrows, with the new residue indicated.

because the membrane spanning domains of bacterial photosynthetic reaction centers are known to form α-helices (1, 7, 49).

To test the requirement for sequence conservation in the fusion peptide of the F protein of SV5 for biological activity, mutations were introduced into the F cDNA to alter both invariant and variant amino acids. In addition, as glycine is a known α-helix destabilizing residue (26), the three glycines in the fusion peptide were converted to alanine residues, a change that has the propensity to increase the α-helical nature of a peptide (59).

MATERIALS AND METHODS

Cells and viruses. Monolayer cultures of the TC7 subclone of CV-1 cells (42) were grown in Dulbecco's modified Eagle's medium (DME) containing 10% NU-Serum IV (Collaborative Research Laboratories, Inc., Bedford, Mass.). Cells were infected with SV40 recombinant virus and SV5 (W3A strain) as described previously (38).

Construction of mutant F proteins and SV40 recombinant viruses. The SV40 late region replacement vector containing the SV5 F cDNA (pSV103F) has been described previously (38). The Asp-718–*Bam*HI fragment from pSV103-F, which contains SV40 sequences and F sequences encoding the fusion peptide, was subcloned into bacteriophage M13 and used for oligonucleotide-directed mutagenesis as described previously (41). The template single-stranded DNA for mutagenesis was uracil enriched (23), and mutagenesis was done as described previously (18). Oligonucleotides were synthesized by the Northwestern University Biotechnology Facility on a DNA synthesizer (model 380B; Applied Biosystems, Inc., Foster City, Calif.). DNA fragments bearing mutations in the desired site were excised from the bacteriophage M13 replicative form by endonuclease digestion and reconstructed into the pSV103 shuttle vector. All mutations were confirmed by direct dideoxynucleotide chain termination sequencing (51) of the double-stranded DNA in the SV40 vectors. The pSV103-F DNAs were introduced into CV-1 cells together with an SV40 early region deletion mutant helper (*dl*1055), and recombinant SV40 virus stocks were prepared as described previously (38, 56).

Radioisotopic labeling, immunoprecipitations, endo-β-*N*-acetylglucosaminidase H (endo H) digestion, immunoblotting, SDS-PAGE, and quantitation of autoradiograms. SV40-F recombinant virus-infected CV-1 cells were labeled with 20 to 50 μCi of Tran^{35}S-label (ICN Radiochemicals Inc., Irvine, Calif.) per ml at 40 to 48 h postinfection (p.i.) for 1 to 2 h in DME deficient in methionine and cysteine (DME Met$^-$ Cys$^-$). Cells were lysed in ice-cold RIPA buffer (25) containing protease inhibitors (1 mM phenylmethylsulfonyl fluoride and 20 ng of aprotinin per μl). For pulse-chase experiments, cells were washed twice in phosphate-buffered saline (PBS), incubated in prewarmed DME Met$^-$ Cys$^-$ for 30 min, and then labeled with 200 μCi of Tran^{35}S-label per ml for the pulse period indicated. The chase period was initiated by removal of the labeling medium, washing, and replacement with prewarmed chase medium (DME supplemented with 2 mM unlabeled cysteine and methionine and 2% NU-Serum IV), and the cells were incubated for various periods. Cells were lysed in ice-cold RIPA buffer containing protease inhibitors and 25 mM iodoacetamide.

F polypeptides were immunoprecipitated from cell lysates by using a rabbit antiserum raised against a mixture of three synthetic peptides specific for F_2 residues 22 to 39, 31 to 46, and 77 to 94; this antiserum was kindly provided by Reay Paterson. Immunoprecipitations were performed as described previously (25). To test for conversion of N-linked carbohydrate chains from the high-mannose form to the complex form, immune complexes on protein A-Sepharose beads were digested with 1 mU of endo H (Boehringer-Mannheim Biochemicals, Indianapolis, Ind.) as described previously (33).

Polypeptides were analyzed by sodium dodecyl sulfate-polyacrylamide gel electrophoresis (SDS-PAGE) on 15% gels in the presence or absence of dithiothreitol, and gels were processed for fluorography as described previously (24). Autoradiograms were quantitated by using a laser

densitometer (LKB Ultrascan; Pharmacia, Inc., Piscataway, N.J.) equipped with LKB Gelscan SL software.

For immunoblotting experiments, SV40 recombinant virus-infected cells were lysed directly on the culture dish with 500 μl of SDS-PAGE lysis buffer containing 2% dithiothreitol, transferred to microcentrifuge tubes, and boiled for 5 min, and samples were sonicated with a microtip sonifier (model 450; Branson Ultrasonics Corp., Danbury, Conn.) to shear DNA. Polypeptides were separated by SDS-PAGE and transferred to nitrocellulose. The nitrocellulose sheet was incubated in 5% nonfat milk solution and then incubated with F_2-specific antiserum diluted in 4% bovine serum albumin (BSA)–PBS. The nitrocellulose filter was washed twice with PBS and twice with PBS containing Tween 20 (Sigma Chemical Co., St. Louis, Mo.), incubated with ^{125}I-goat anti-rabbit immunoglobulin G (IgG) as secondary antibody, washed as before, and autoradiographed.

Immunofluorescence microscopy and flow cytometry. SV40 recombinant virus-infected CV-1 cells grown on glass coverslips were prepared for cell surface staining by fixation in PBS containing 0.1% methanol-free formaldehyde (Polysciences, Inc., Warrington, Pa.) for 10 min at room temperature, followed by washing in PBS. Monoclonal antibody (MAb) F1a, specific for the SV5 F glycoprotein and kindly provided by Rick Randall, University of St. Andrews, St. Andrews, Fife, Scotland (43), was used as the primary antibody at a 1:500 dilution in 1% BSA–PBS, and fluorescein isothiocyanate-conjugated goat anti-mouse IgG (Organon Teknika-Cappel, Malvern, Pa.) was used as the secondary antibody. Incubation conditions for immunofluorescence microscopy were used as described previously (9), and cells were photographed with a Nikon Microphot-FXA microscope system (Nikon Corp., Tokyo, Japan).

For flow cytometry, culture dishes (6 cm) of SV40 recombinant virus-infected CV-1 cells were chilled on ice, and the cells were washed with ice-cold PBS containing 0.02% sodium azide (PBSN). MAb F1a was added to the monolayer at 1:500 dilution in PBSN containing 1% BSA, and the mixture was incubated on the plate for 30 min at 4°C. The cell monolayers were washed five times with PBSN, incubated with fluorescein isothiocyanate-conjugated goat anti-mouse IgG for 30 min at 4°C, and washed five times with PBSN and two times with PBS deficient in calcium and magnesium (PBS^-) to remove unbound secondary antibody. To remove cells from the dish, PBS containing 50 mM EDTA (0.5 ml) was added and cells were incubated at 4°C until they dissociated easily from the plate with aspiration. Cells were transferred to flow cytometry tubes containing 0.5 ml of 1% methanol-free formaldehyde and dispersed by pipetting. Fluorescence intensity of 10,000 cells was measured by a FACSCAN flow cytometer (Becton Dickinson, Mountain View, Calif.).

Assessment of extent of fusion and antibody-mediated inhibition of syncytium formation. Mutant F proteins expressed by using SV40-recombinant viruses were assessed for the ability to mediate syncytium formation in CV-1 cells as described previously (38). Syncytia were photographed at 48 h p.i. by using a Nikon Diaphot inverted phase-contrast microscope and Kodak T-MAX film (Eastman Kodak Co., Rochester, N.Y.).

To inhibit syncytium formation, CV-1 cells infected with SV40 recombinant viruses were washed at 24 h p.i. with PBS, and the medium was replaced with 2 ml of DME–2% NU-Serum IV containing a 1:50 dilution of MAb F1a ascites fluid. Cells were incubated for a further 24 h. As a control for nonspecific inhibition, an irrelevant antibody (MAb 14C2 specific for the influenza virus M_2 protein ectodomain [68]) was overlaid onto parallel plates at equal dilution.

Measurement of the area of the syncytia caused by the different SV40 recombinant viruses was facilitated by using Sigma Scan scientific measurement system hardware and software (Jandel Scientific, Corte Madera, Calif.). Photomicrographs of syncytium-containing fields (at least three fields of 1.04×10^6 μm^2 in area, totalling 7 to 70 syncytia per recombinant virus stock) of cells were enlarged to optimize accurate tracing of the syncytia during electromagnetic digitization of the images. A scale calibration standard was provided by enlargement of the image of a stage micrometer photographed under identical conditions.

RESULTS

Mutagenesis rationale and expression of the altered F proteins. To test the requirements for sequence conservation in the paramyxovirus F_1 protein N-terminal domain, selected mutations were made in the F peptide by oligonucleotide-directed mutagenesis of a cDNA clone of the paramyxovirus SV5 F gene. The mutants contained the following changes: hydrophobic residues substituted for different hydrophobic residues (F_1L, V_5L, $A_{10}V$, and $V_{13}I$, using a nomenclature system in which the first letter specifies the original residue, the number specifies its position in the fusion peptide, and the following single letter specifies the substituted residue), a polar residue changed to an aliphatic residue ($T_{15}V$), conversion of the three glycine residues to alanine which should theoretically make the fusion peptide more α-helical (G_3A, G_7A, and $G_{12}A$), shortening of the length of the hydrophobic sequence by introduction of a charged residue at position 12 or 18 ($G_{12}E$, $Q_{18}E$, and $Q_{18}K$), and substitution of glutamine by asparagine ($Q_{18}N$), which also adds a site for the potential addition of N-linked carbohydrate. In addition, two more radical changes were made: mutant $A_{10}V$-$G_{12}A$-$A_{14}I$ (V_{10} $A_{12}I_{14}$) contains three changes and makes the fusion peptide slightly more hydrophobic, and mutant $TAVGLA_{10-15}$ contains a reversal of the order of the conserved sequence of residues 10 to 15 (Fig. 1A). The change F_1L occurs naturally in the F protein of some strains of Newcastle disease virus (60), so this change was not expected to cause a large difference in phenotype. The single-residue changes are shown in Fig. 1B, with the fusion peptide sequence modeled as an α-helix. It can be seen that the mutations involve residues that are on both the variant and invariant face of the putative helix.

The altered F cDNAs were expressed in CV-1 cells by using an SV40 late-region replacement vector as described previously (38, 41). SV40 recombinant virus-infected cells were labeled for 30 min with Tran^{35}S-label, immunoprecipitated with anti-F specific serum, and analyzed by SDS-PAGE. As shown in Fig. 2, an F_0 polypeptide with a mobility similar to that of wild-type (wt) F_0 was expressed by all the mutants with the exception of $Q_{18}N$. Mutant $Q_{18}N$ synthesized an F_0 of slightly slower mobility than wt F_0, and this size difference (~3 kDa) is compatible with that expected for a carbohydrate chain added to the asparagine residue at the newly created site (NVT) for N-linked carbohydrate addition. Synthesis of $Q_{18}N$ and wt F in the presence of tunicamycin, an inhibitor of N-linked glycosylation, yielded F proteins of identical mobility, indicating that the newly created site for N-linked glycosylation is utilized (data not shown). Detection of the F_1 polypeptide, an F_0 cleavage product, was hindered because it comigrates with the SV40 VP1 polypeptide that precipitates nonspecifically in immu-

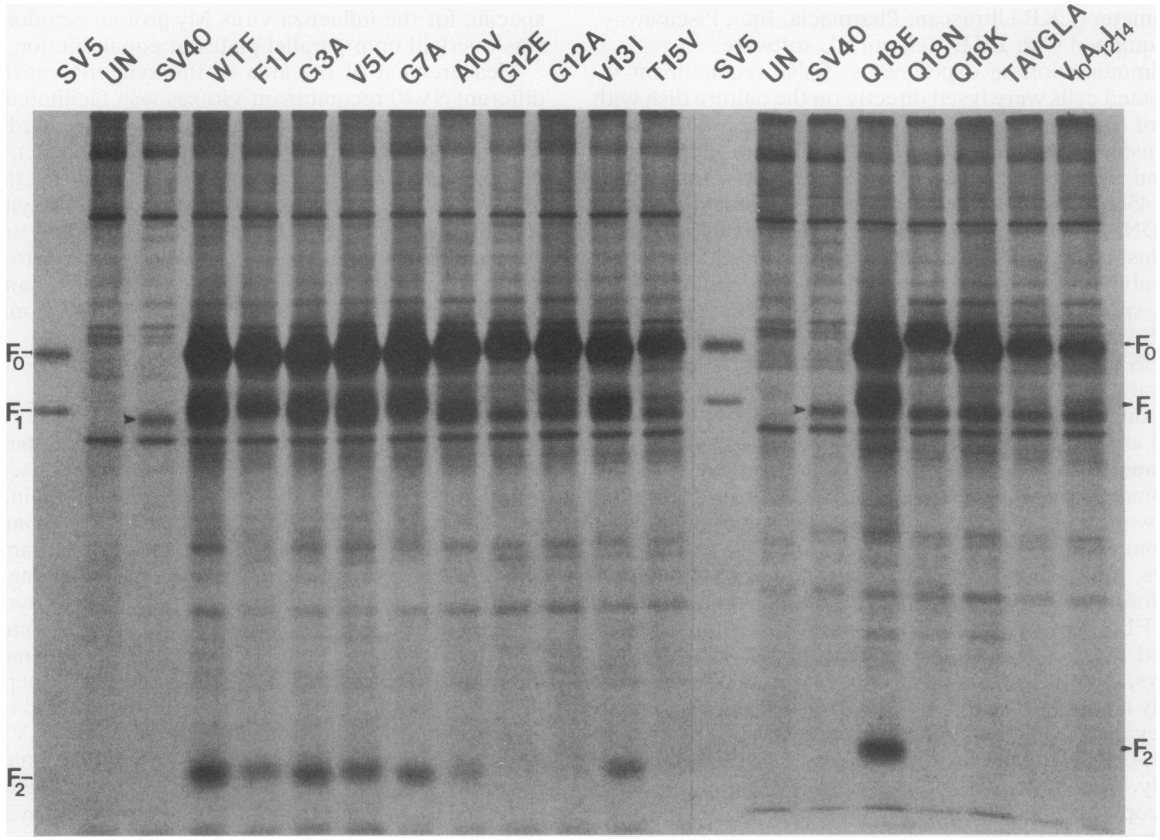

FIG. 2. Expression of the mutant F proteins. Recombinant SV40 F virus-infected CV-1 cells were labeled with 50 μCi of Tran^{35}S-label per ml for 2 h at 36 h p.i., and polypeptides were immunoprecipitated with F_2-specific antiserum. Polypeptides were analyzed by SDS-PAGE in the presence of reducing agent. The positions of the uncleaved F_0 and the subunits F_1 and F_2 are indicated. Arrowhead indicates the SV40 VP1 polypeptide which precipitates nonspecifically and comigrates with the F_1 subunit. SV5, F_0, F_1, and F_2 immunoprecipitated from SV5-infected CV-1 cells. UN, uninfected CV-1 cells. SV40, wt SV40. The nomenclature of the mutants follows that indicated in the text with the first single letter specifying the original residue, the number specifying its position in the fusion peptide, and the following single letter specifying the substituted residue. $V_{10}A_{12}I_{14}$ contains the following changes: $A_{10}V$, $G_{12}A$, $A_{14}I$, and mutant $TAVGLA_{10-15}$ contain a reversal of the order of the conserved residues 10 to 15 (Fig. 1).

noprecipitation assays. Nonetheless, F_1 could be readily detected with mutants F_1L, G_3A, V_5L, G_7A, $A_{10}V$, $V_{13}I$, and $Q_{18}E$. Small amounts of F_1 could be detected with mutants $G_{12}A$, $T_{15}V$, and $V_{10}A_{12}I_{14}$. No detectable F_1 was observed with mutants $G_{12}E$, $Q_{18}N$, and $Q_{18}K$. However, the other cleavage product, the F_2 polypeptide, could only be detected with mutants F_1L, G_3A, V_5L, G_7A, $A_{10}V$, $V_{13}I$, and $Q_{18}E$ but not with mutants $G_{12}A$, $G_{12}E$, $T_{15}V$, $Q_{18}N$, $Q_{18}K$, $V_{10}A_{12}I_{14}$, and $TAVGLA_{10-15}$. As described below, the very small amount of cleavage of $T_{15}V$ and $V_{10}A_{12}I_{14}$ did not make the cleaved population amenable to further characterization. However, the cleaved population of $G_{12}A$ had altered biological activity (see below).

Cleavage of the SV5 F_0 precursor polypeptide to the disulfide-linked polypeptides F_1 and F_2 goes nearly to completion (Fig. 3B and reference 42). Thus, cleavage of SV5 F_0 to F_1 and F_2 is an excellent indicator of intracellular transport. With the Newcastle disease virus F protein, cleavage also occurs late after synthesis, and it has been suggested that cleavage of F_0 occurs in the *trans*-Golgi apparatus or *trans*-Golgi network (32, 50). The rate of intracellular transport of SV5 wt F expressed from the SV40 vector has not been reported, but cell surface antibody binding studies show it occurs before arrival at the cell surface (36). Thus, the rate at which carbohydrate chains obtained resistance to digestion with endo H, indicative of transport to the medial Golgi, and its temporal relationship to F cleavage were determined. SV40 wt F recombinant virus-infected CV-1 cells were pulse-labeled with Tran^{35}S-label for 10 min and incubated for various periods. Polypeptides were immunoprecipitated, treated with or without endo H, and analyzed by SDS-PAGE. Samples were subjected to electrophoresis under nonreducing conditions to examine the endo H-sensitive and -resistant species (as F_0 and $F_{1,2}$ migrate as a single band on the gel) and under reducing conditions to examine the cleaved products. As shown in Fig. 3A, the F-related species acquired resistance to digestion with endo H with a half-life ($t_{1/2}$) ≈ 45 min, and by 120 min nearly all detectable F species were resistant to endo H digestion, indicating the vast majority of F was transported to the medial Golgi apparatus. The kinetics of cleavage ($t_{1/2}$ ≈ 65 min) (Fig. 3B) indicated that proteolytic cleavage of F_0 occurs in an intracellular compartment after the medial Golgi apparatus during exocytosis. The mature SV5 F protein contains six potential sites for addition of N-linked carbohydrates, four on the F_1 subunit and two on the F_2 subunit (37). The data shown in Fig. 3B indicate that whereas F_1 carbohydrate chains acquire endo H resistance (F_1 resistant to endo H [F_{1R}]

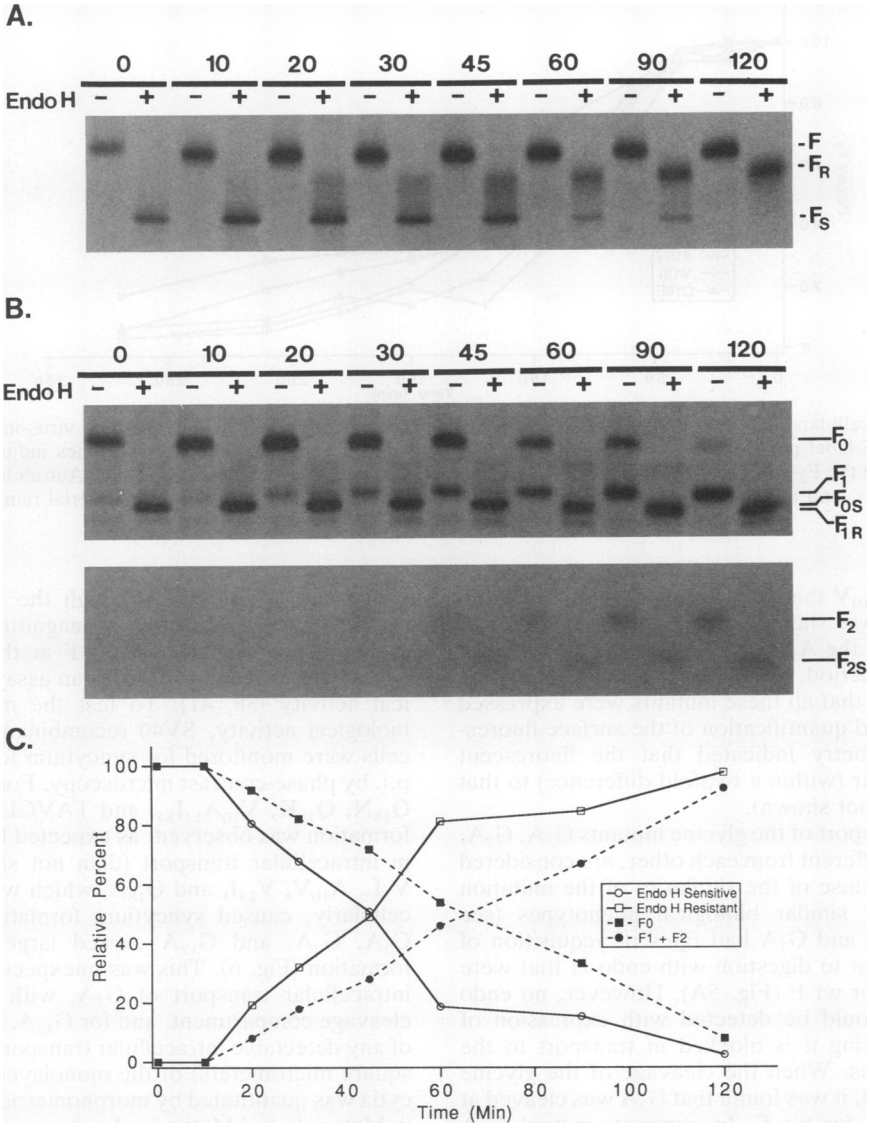

FIG. 3. Intracellular transport and cleavage of the SV5 F protein. SV40 wt F recombinant virus-infected CV-1 cells were labeled with 200 μCi of Tran^{35}S-label per ml for 10 min at 40 h p.i. and incubated in chase medium for the times indicated. Polypeptides were immunoprecipitated with F_2-specific antiserum and treated (+) or not treated (−) with endo H. (A) SDS-PAGE in the absence of reducing agent. F, position of the untreated disulfide-linked heterodimer of $F_1 + F_2$ and F_0; F_S, endo H-sensitive form of F; F_R, endo H-resistant form of F. (B) Samples similar to those shown in panel A were analyzed by SDS-PAGE in the presence of reducing agent. F_0, untreated F_0; F_1, untreated F_1; F_2, untreated F_2. F_{0S}, F_{1R}, and F_{2S}, endo H-sensitive (S) or resistant (R) species of the polypeptides. (C) Quantitation by densitometric analysis of the autoradiograms shown in panels A and B. Data are plotted as the percentage of the total F-specific radioactive material in each lane of the gel.

comigrates with F_0 sensitive to endo H digestion [F_{0S}]), a mobility shift is observed between F_1 and F_{1R}, suggesting that one of the carbohydrate chains on F_1 remains in the high-mannose form. The carbohydrate chains on F_2 remain in the high-mannose form and are not modified to a complex carbohydrate form.

Analysis of the rate of intracellular transport of the fusion peptide mutants. To examine the intracellular transport of the F proteins with altered residues in the fusion peptides, the rate of acquisition of carbohydrate chains resistant to endo H digestion and the rate of cleavage of F_0 to F_1 and F_2 were determined. For mutants $G_{12}E$, $T_{15}V$, $Q_{18}N$, $Q_{18}K$, $V_{10}A_{12}I_{14}$, and $TAVGLA_{10-15}$, acquisition of carbohydrate chains resistant to endo H digestion could not be detected and no conversion of F_0 to F_1 and F_2 was observed. In addition, no surface expression of these mutant F molecules could be detected by immunofluorescent staining with an anti-F MAb (data not shown; see Fig. 2 for single time point of cleavage). These data indicate that these mutations cause an alteration to the F molecules that blocks intracellular transport to the medial Golgi apparatus.

Mutants F_1L, V_5L, $A_{10}V$, $V_{13}I$, and $Q_{18}E$ all showed rates of acquisition of carbohydrate chains resistant to endo H digestion that were very similar to that for wt F (data not shown). The rate of cleavage of F_0 to F_1 and F_2 was also similar to that for wt F except for mutant $A_{10}V$ (Fig. 4). For

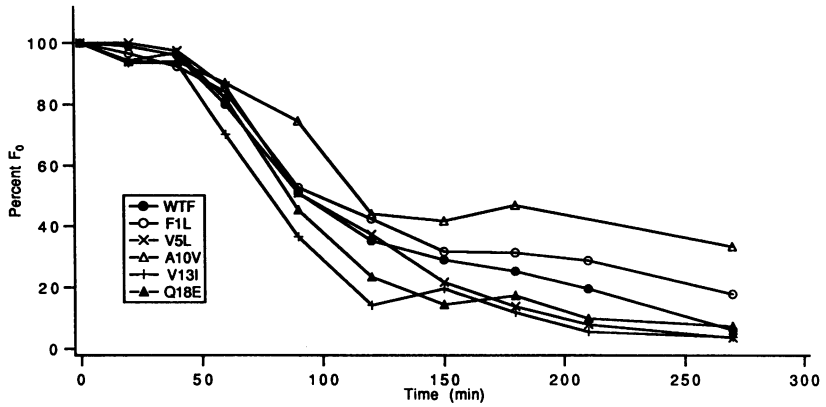

FIG. 4. Rate of intracellular transport of F mutants to the cleavage compartment. SV40 F recombinant virus-infected cells were labeled with 200 μCi of Tran^{35}S-label per ml at 40 h p.i. for 10 min and incubated in chase medium for the times indicated. Polypeptides were immunoprecipitated with the F_2-specific antiserum and analyzed by SDS-PAGE under reducing conditions. Autoradiograms were quantitated by densitometric analysis, and the data were plotted as the percentage of total F-specific radioactive material remaining as F_0.

those molecules of $A_{10}V$ that were cleaved (~70% of total) the rate of cleavage was slightly slower than that for wt F. The remaining 30% of the $A_{10}V$ molecules were not cleaved in a 270-min chase period. Fluorescent staining with the anti-F MAb indicated that all these mutants were expressed at the cell surface, and quantification of the surface fluorescence by flow cytometry indicated that the fluorescent intensities were similar (within a twofold difference) to that found for wt F (data not shown).

The kinetics of transport of the glycine mutants G_3A, G_7A, and $G_{12}A$, although different from each other, are considered together not only because of the similarity of the mutation but because of their similar biological phenotypes (see below). Mutants G_3A and G_7A had rates of acquisition of carbohydrates resistant to digestion with endo H that were very similar to that for wt F (Fig. 5A). However, no endo H-resistant species could be detected with expression of mutant $G_{12}A$, suggesting it is blocked in transport to the medial Golgi apparatus. When the cleavage of the glycine mutants was examined, it was found that G_3A was cleaved at a rate similar to that for wt F. In contrast, mutant G_7A seemingly consisted of a population of molecules that was cleaved with somewhat slower kinetics than those of wt F and a population of G_7A molecules that remained uncleaved in a 270-min chase period. As expected from the lack of resistance to endo H, no cleavage of $G_{12}A$ could be detected (Fig. 5B). The kinetic analysis of G_7A transport was complicated by the finding that between 60 and 90 min after the pulse-label, the total amount of endo H-resistant G_7A and the amount of both uncleaved and cleaved G_7A declined, indicating G_7A is relatively unstable compared with wt F (Fig. 5C). From the quantitation of the rates of resistance of G_7A to endo H digestion, cleavage, and stability, it can be deduced that degradation of G_7A approximately coincides with the time of F cleavage. This finding that the cleaved F_1 and F_2 of mutant G_7A are unstable may cause an exaggeration of the amount of F_0 found to remain after the 120-min chase period (Fig. 5B), because the quantitation is based on the amount of the total F species represented by F_0 at each of the specific single time points. The cell surface expression of the glycine mutants is described below.

Fusion activity of the fusion peptide mutants. We have shown previously that the SV5 F protein, when expressed in CV-1 cells by using a recombinant SV40 F virus, causes syncytium formation. Although the number of detectable syncytia is several orders of magnitude less than the large number of cells that express F at the plasma membrane, syncytium formation provides an assay for F protein biological activity (38, 41). To test the mutant F proteins for biological activity, SV40 recombinant virus-infected CV-1 cells were monitored for syncytium formation at 48 to 50 h p.i. by phase-contrast microscopy. For mutants $G_{12}E$, $T_{15}V$, $Q_{18}N$, $Q_{18}K$, $V_{10}A_{12}I_{14}$, and $TAVGLA_{10-15}$, no syncytium formation was observed, as expected for F proteins blocked in intracellular transport (data not shown). Mutants F_1L, V_5L, $A_{10}V$, $V_{13}I$, and $Q_{18}E$, which were transported intracellularly, caused syncytium formation (Fig. 6). Mutants G_3A, G_7A, and $G_{12}A$ caused large areas of syncytium formation (Fig. 6). This was unexpected given the impaired intracellular transport of G_7A, with its instability in the cleavage compartment, and for $G_{12}A$, with the seeming lack of any detectable intracellular transport. The surface area (in square micrometers) of the monolayer covered by the syncytia was quantitated by morphometric analysis as described in Materials and Methods. As shown in Fig. 7, expression of mutants F_1L, V_5L, $A_{10}V$, $V_{13}I$, and $Q_{18}E$ did not cause a large difference in the percentage of the area of CV-1 cell monolayers that was involved in syncytium formation versus that observed with wt F expression (fusion of wt F = 3%). However, mutants G_3A, G_7A, and $G_{12}A$ caused 16.6, 37.4, and 47.2%, respectively, of the monolayer area to be involved in syncytium formation (Fig. 7).

Cleavage and cell surface expression of mutants G_3A, G_7A, and $G_{12}A$. Although intracellular transport of G_7A was impaired and $G_{12}A$ could not be detected in the metabolic labeling experiments, the fusion observed made it important to use a more sensitive immunoblotting assay to search for an accumulation of cleaved F molecules. Equal amounts of lysates from cells expressing wt F, G_3A, G_7A, $G_{12}A$, and V_5L were subjected to SDS-PAGE. In alternating lanes of the gel, uninfected cell lysates were analyzed. The polypeptides were transferred to nitrocellulose membranes and immunoblotted by using anti-F_2 serum and ^{125}I-labeled secondary antibody. As shown in Fig. 8, the amounts of F_2 that accumulated in cells expressing wt F, G_3A, and V_5L were similar. Most importantly, although present in greatly reduced amounts, some F_2 accumulation was detected in cells expressing mutants G_7A and $G_{12}A$. The amount of $G_{12}A$ is

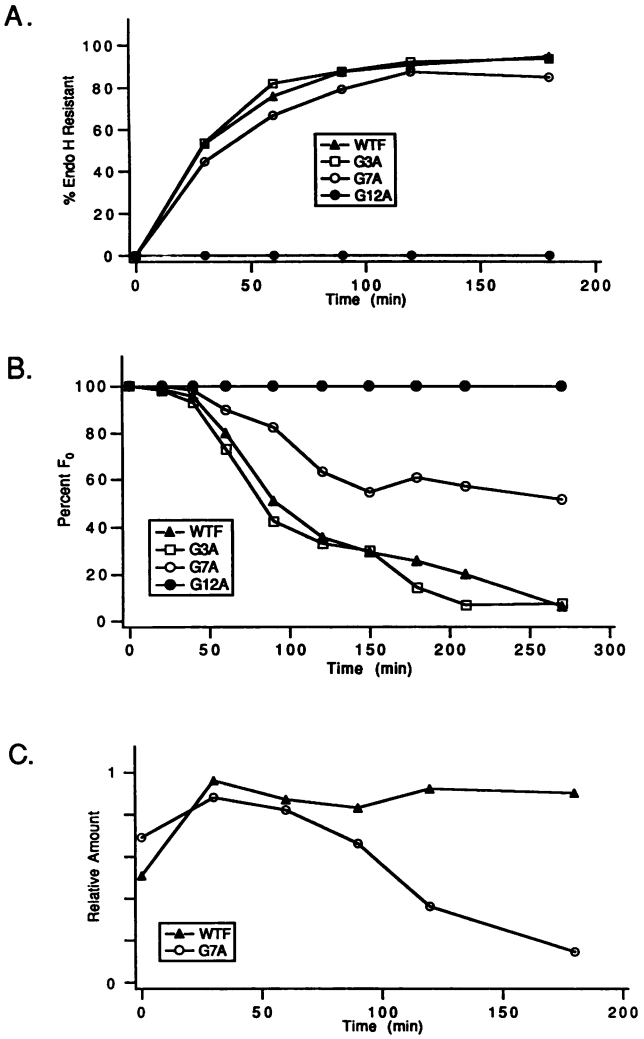

FIG. 5. Rate of intracellular transport of the F glycine mutants to the medial Golgi apparatus and the cleavage compartment. SV40 F recombinant virus-infected cells, expressing mutants G_3A, G_7A, and $G_{12}A$, were labeled with 200 μCi of Tran^{35}S-label per ml at 40 h p.i. for 10 min and incubated in chase medium for the times indicated. Polypeptides were immunoprecipitated with the F_2-specific antiserum, treated with or without endo H, and analyzed on SDS-PAGE under nonreducing and reducing conditions. Autoradiograms were quantitated by densitometric analysis. (A) Rates of acquisition of F carbohydrate chains resistant to digestion with endo H. Samples were analyzed on gels under nonreducing conditions; data are plotted as the percentage of endo H-resistant species, as in Fig. 3. (B) Rates of cleavage of F_0 to F_1 and F_2. Samples were analyzed on gels under reducing conditions. Data are plotted as the percent of total F-specific species remaining as F_0. (C) Stability of F mutant G_7A polypeptide. The relative amounts of F-specific species of both wt F and mutant G_7A are indicated in arbitrary units.

slightly greater than that of G_7A even though in the kinetic analysis cleavage of $G_{12}A$ to F_1 and F_2 was not detected whereas G_7A cleavage products were readily detected (Fig. 5B). This can be explained because in the blot analysis, accumulation of F species synthesized over 48 h is analyzed and a large proportion of G_7A is degraded at a time point almost coincident with cleavage (Fig. 5C).

To examine for cell surface expression of G_3A, G_7A, and $G_{12}A$, the cell surface was stained with the anti-F MAb. Whereas cells expressing wt F or G_3A exhibited a bright surface staining pattern, those expressing G_7A and $G_{12}A$ showed a much weaker and diffuse staining pattern (Fig. 9A). This decreased fluorescent staining is unlikely to be due to differences in reactivity of the mutant proteins for the F1a MAb, as very similar data was obtained by using an F-specific polyclonal rabbit sera (data not shown). Quantitation of the relative F1a-specific surface fluorescence intensity by flow cytometry demonstrated intense fluorescence for wt F and G_3A and greatly reduced staining for mutants G_7A and $G_{12}A$ (G_7A is 15% of wt F and $G_{12}A$ is 23% of wt F [Fig. 9B]). Thus, the cell surface staining intensity of G_7A and $G_{12}A$ in comparison to wt F, like the amount of F_2 that accumulated, correlated inversely with increased fusion activity of the mutants.

F MAb inhibition of syncytium formation. It has been shown previously that antibody to F protein can inhibit cell-to-cell fusion (29, 30) and cause virus neutralization (40, 43). To show that the fusion observed in cells expressing G_3A, G_7A, and $G_{12}A$ was due to F molecules that were expressed at the cell surface and was not due to trivial causes, the F1a MAb was added to CV-1 cells infected with the SV40 F recombinant viruses at 24 h p.i., a time when no fusion could be detected. As a control for nonspecific effects, ascites fluid of an irrelevant MAb (14C2, specific for the ectodomain of influenza A virus M_2 protein [68]) was used. As shown in Fig. 10, whereas the control cells showed extensive syncytium formation at 48 h p.i., the F MAb inhibited fusion. The low-power-magnification photograph of the cells incubated without antibody is shown (Fig. 10) to illustrate better the extent of syncytium formation across a greater area of cells.

DISCUSSION

Although virus-mediated cell fusion is a phenomenon that has been observed over many decades, little is known about the mechanistic details of the initial interactions between the viral fusion proteins and the lipid bilayer which lead to membrane coalescence. Several viral fusion proteins share the common feature of requiring proteolytic processing for activation of the fusion activity and have a hydrophobic domain following the newly released N terminus that is relatively glycine rich, e.g., influenza virus HA_2 N-terminal region and human immunodeficiency virus gp41 and simian immunodeficiency virus (SIV) gp32 N-terminal regions (4, 11, 12). With the paramyxoviruses, cleavage of the F protein generates a new N terminus on the F_1 subunit, and it has been speculated that the released highly conserved hydrophobic fusion peptide domain can disrupt membrane integrity by direct interaction with the lipid bilayer (13, 34, 54). To examine the effect of alterations in the conserved fusion domain on syncytium formation, site-specific mutations (summarized in Table 1) were made in the paramyxovirus SV5 F protein fusion peptide.

The biological activity of the F protein as determined by syncytium formation can only be measured if the F protein is expressed at the cell surface. Over the past several years it has been established for several integral membrane proteins that proper folding and oligomerization are prerequisites for transport from the endoplasmic reticulum (ER) to the Golgi cisternae (reviewed in reference 48). Many point mutations have been shown to lead to malfolded proteins that are retained in the ER. However, some mutants are efficiently exported from the ER but they are still blocked in transport to the cell surface: mutants in the cytoplasmic tail of

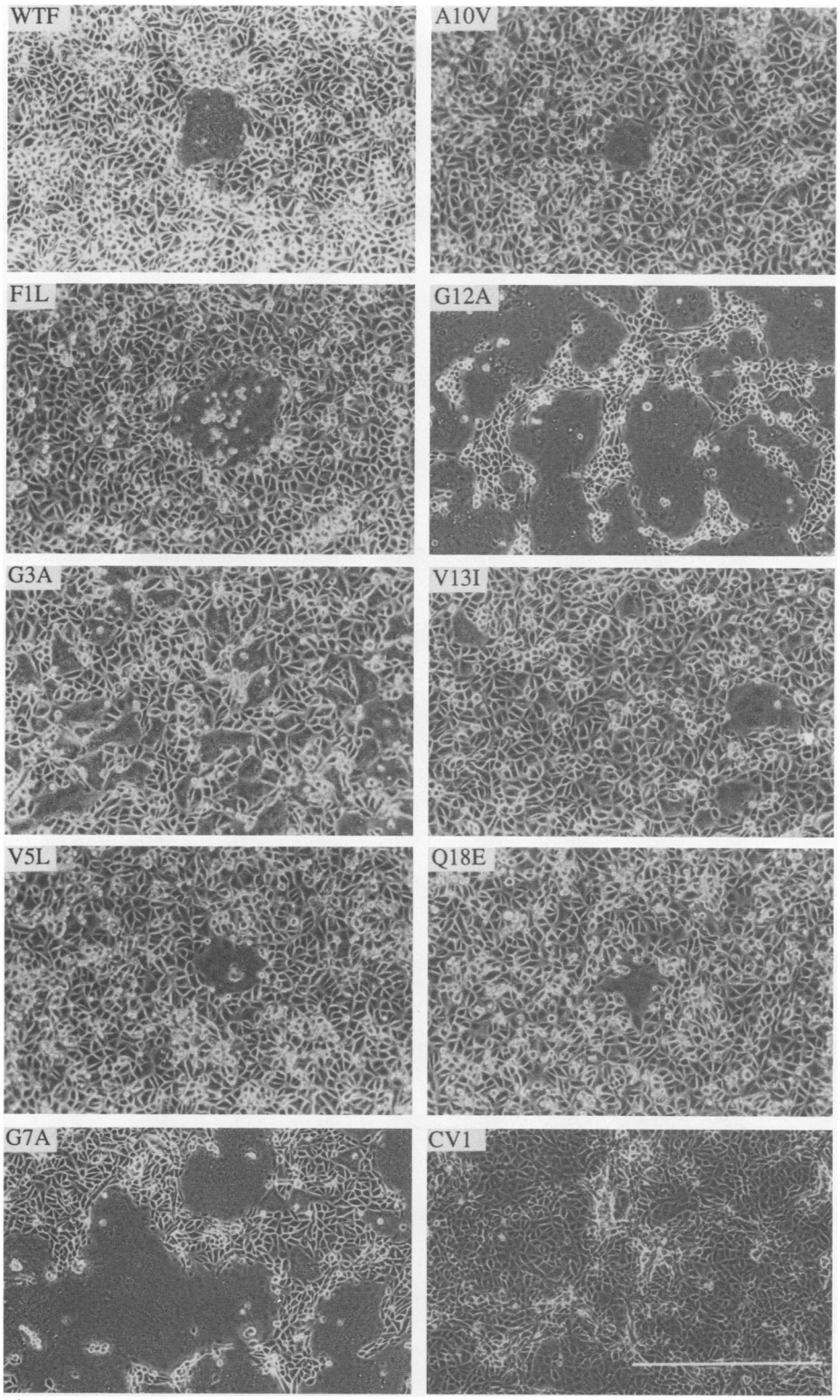

FIG. 6. Syncytium formation by the mutant F proteins. SV40 F recombinant virus-infected CV-1 cells expressing wt F and the mutants indicated were photographed at 48 h p.i. Typical syncytia observed for all of the fusion-inducing mutants are shown. CV-1, uninfected CV-1 cells. Bar = 500 μm.

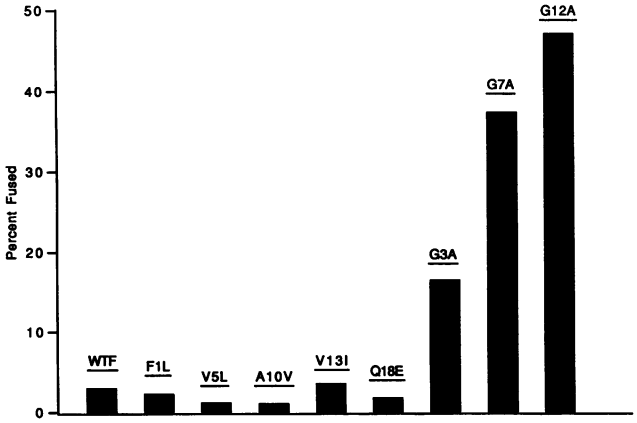

FIG. 7. Quantitation of the extent of fusion. The area of syncytia over photographic fields of 1.04×10^6 μm^2 was measured as described in Materials and Methods.

influenza virus hemagglutinin (HA) (8), vesicular stomatitis virus G proteins (47), and an SV5 HA-neuraminidase protein with altered membrane-flanking regions (35) all exhibit this phenotype. The SV5 F fusion peptide mutants described here, although mostly involving single-amino-acid substitutions, exhibited varied transport properties ranging from unaltered F transport rates ($t_{1/2} \approx 65$ min to F cleavage compartment) (F_1L, G_3A, V_5L, $A_{10}V$, $V_{13}I$, and $Q_{18}E$) to incomplete transport to the cell surface (G_7A and $G_{12}A$) and to undetectable transport to the medial Golgi apparatus ($G_{12}E$, $T_{15}V$, $Q_{18}N$, $Q_{18}K$, $V_{10}A_{12}I_{14}$ and $TAVGLA_{10-15}$). The block in transport suggests that some of these mutations

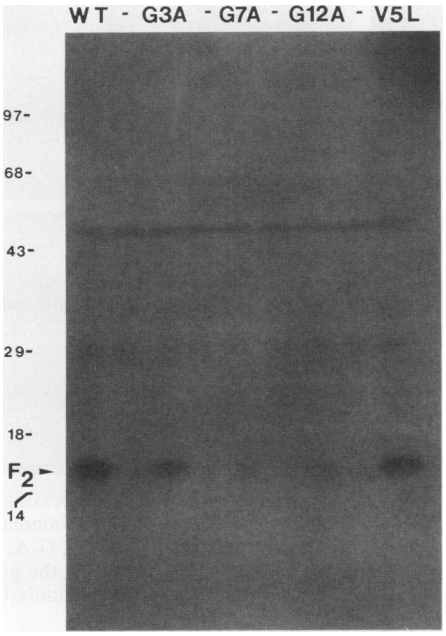

FIG. 8. Immunoblot analysis of the accumulation of F_2 of the glycine mutants. Equal amounts of lysates of cells infected with the SV40 F recombinant viruses and uninfected cell lysates (lanes −) were separated by SDS-PAGE, and the polypeptides were transferred to a nitrocellulose filter. The filter was incubated sequentially with F_2-specific serum and ^{125}I-goat anti-rabbit IgG. Numbers indicate 10^3 molecular weight markers, and the position of the F_2 subunit is indicated.

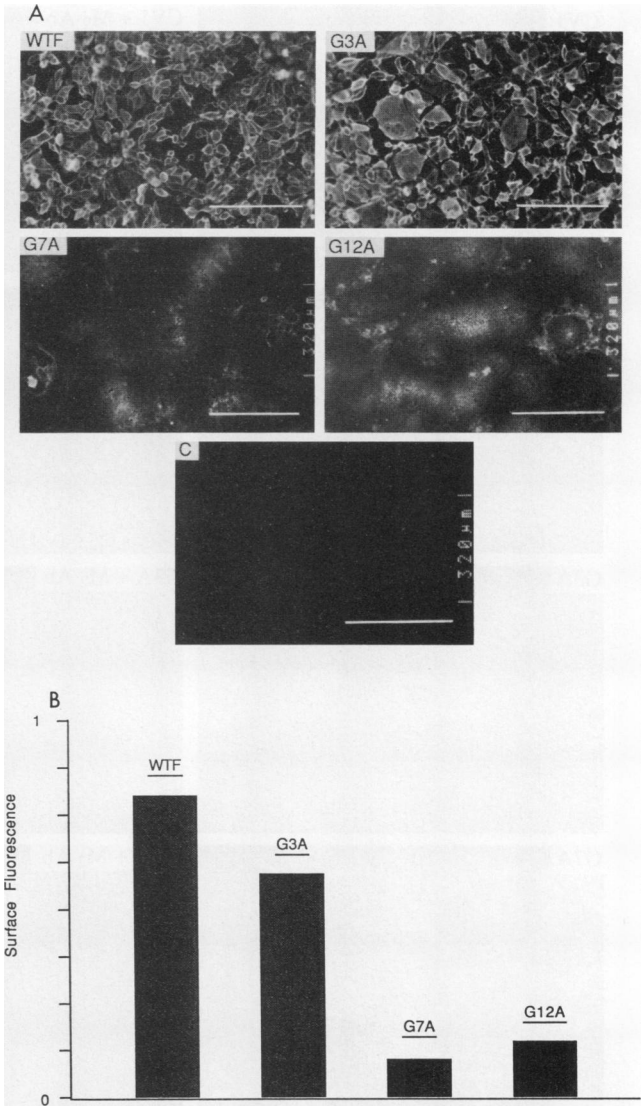

FIG. 9. Cell surface expression of the F glycine mutants. (A) SV40 F recombinant virus-infected cells expressing wt F, G_3A, G_7A, and $G_{12}A$ and cells infected with an irrelevant SV40 recombinant virus (C) (expressing the influenza virus HA glycoprotein) were prepared for cell surface immunofluorescence as described in Materials and Methods. Primary antibody was MAb F1a (43), and secondary antibody was fluorescein isothiocyanate-labeled rabbit anti-mouse IgG. The exposure time for all photographic manipulations were identical for each sample. Bars = 320 μm. (B) SV40 F recombinant virus-infected cells expressing wt F and the glycine mutants G_3A, G_7A, and $G_{12}A$ were processed for flow cytometry as described in Materials and Methods. Primary antibody was MAb F1a (43), and secondary antibody was fluorescein isothiocyanate-labeled rabbit anti-mouse IgG. The total F-specific surface fluorescence for each mutant is indicated as a histogram bar on an arbitrary scale.

may cause profound changes in protein folding. However, other changes may cause local folding defects; such changes were postulated to explain the loss of biological activity of the F protein after residues were altered within the arginine-rich cleavage site (41) and in mutations distant to the cleavage site that caused a difference in the type of serine protease capable of activating the F protein (21).

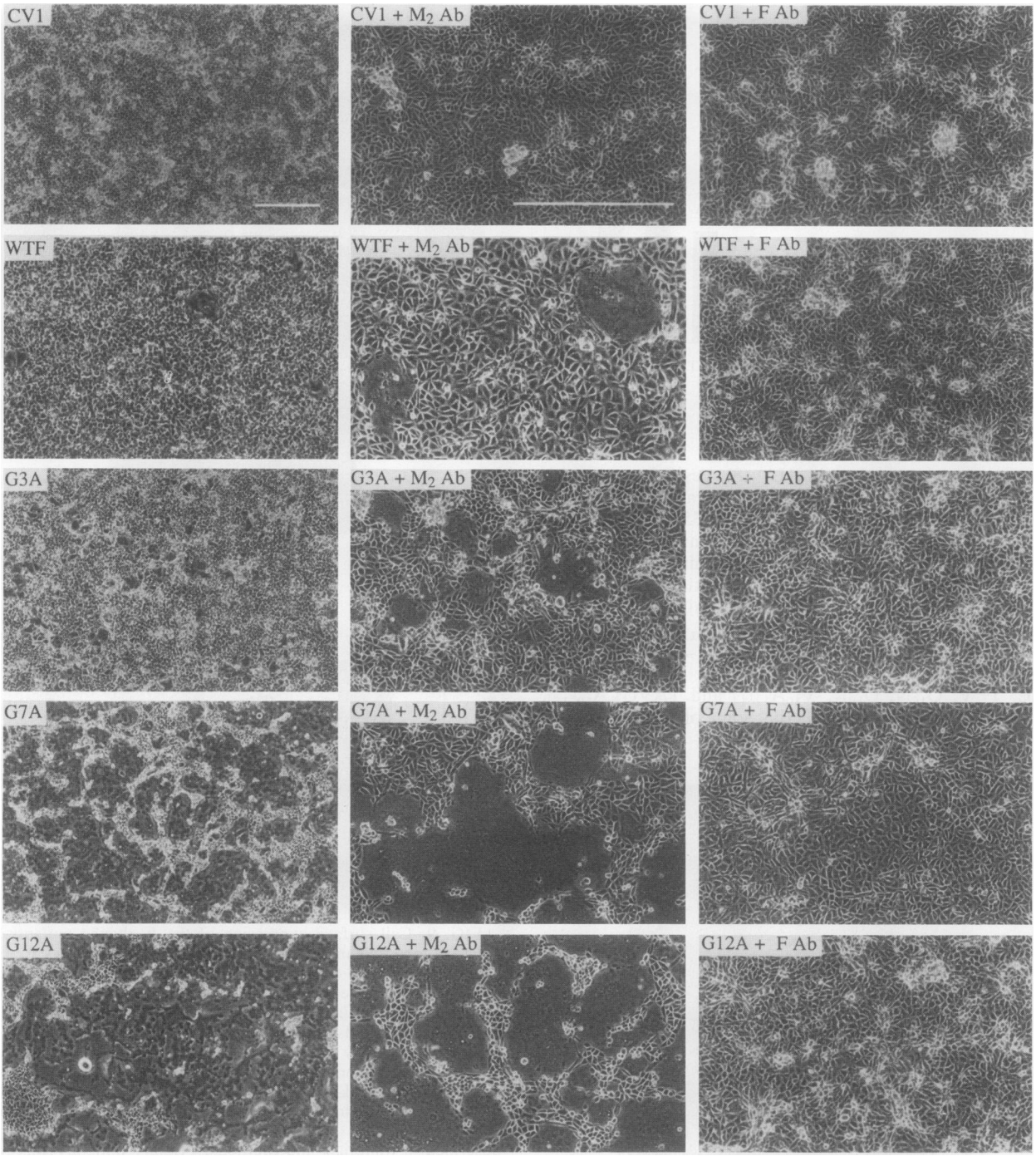

FIG. 10. Syncytium formation is inhibited by MAb to the F protein. SV40 F recombinant virus-infected CV-1 cells expressing wt F and the glycine mutants G_3A, G_7A, and $G_{12}A$ were incubated from 24 to 48 h p.i. with or without MAb to the SV5 F protein, and monolayers were photographed at 48 h p.i. The left panels show low-magnification photographs of typical syncytia induced by the wt F, G_3A, G_7A, and $G_{12}A$ mutants compared to control uninfected cells. The middle panels show photographs of similarly infected cells incubated in the presence of an irrelevant MAb which is specific for the M_2 protein of influenza A virus (+M_2 Ab). The right panels show photographs of similarly infected cells incubated in the presence of MAb specific for the SV5 F protein (+F Ab). Bars = 500 μm.

The observation of sequence identity among the F peptides of paramyxoviruses and the finding that peptides mimicking the sequence of the F peptide inhibit fusion of paramyxoviruses have led to speculation that there is a specific protein or lipid fusion receptor in the target membrane (45). The fact that several of the mutations described here do not affect the ability of F to cause syncytium formation, regardless of whether the substitutions are of a similar or dissimilar nature, makes it less likely that there is a cellular receptor for the F peptide. No SV5 F mutants were

TABLE 1. Properties of the mutant F proteins

Mutant[a]	Transport ($t_{1/2}$)	Surface expression[b]	% Fusion[c]
wt F	75[d]	1.0	3.02
F_1L	90[d]	0.55	2.32
V_5L	75[d]	0.70	1.25
$A_{10}V$	100[d,e]	0.76	1.10
$V_{13}I$	75[d]	1.23	3.60
$Q_{18}E$	90[d]	0.70	1.80
G_3A	45[f]	0.74	16.58
G_7A	50[f]	0.15	37.44
$G_{12}A$	—[g]	0.23	47.20
$G_{12}E$	—	—	—
$T_{15}V$	—	—	—
$Q_{18}N$	—	—	—
$Q_{18}K$	—	—	—
$V_{10}A_{12}I_{14}$	—	—	—
$TAVGLA_{10-15}$	—	—	—

[a] Mutants are designated by the original residue of the fusion peptide and its position from the F_1 N terminus followed by the new residue.
[b] Cell surface F protein-specific fluorescence at 45 h p.i. determined by flow cytometry. Relative values are expressed as normalized to wt F.
[c] Percentage of syncytium-containing field which is fused, determined by morphometric analysis.
[d] $t_{1/2}$ of cleavage of F_0 to $F_1 + F_2$ in minutes.
[e] Approximately 30% of this mutant remains uncleaved after a 2.5-h chase.
[f] $t_{1/2}$ of acquisition of endo H-resistant carbohydrates in minutes.
[g] —, not detectable.

obtained which were transport competent but defective in fusion activity, analogous to the substitution of glutamic acid for glycine at residue 4 of the influenza virus HA_2 F peptide which rendered a transport-competent but fusion-defective molecule (12).

Our quantitation of cell fusion was based on the relative syncytium-inducing capacity observed for the mutant SV5 F proteins when expressed from an SV40 vector. Although viral F proteins do not always induce syncytia, the SV5 F protein causes fusion in many but not all cell types when expressed because of SV5 infection of cells or from vector-based cDNA expression systems (15, 38, 40). It would be ideal to use biochemical fusion assays to monitor the mixing of contents during fusion. Such assays have been developed in which enzymes or fluorescent probes are transferred from a donor membrane-bound compartment to an acceptor compartment; dequenching of the fluorescence of octadecyl rhodamine dye (R18) has been particularly successful for monitoring lipid mixing during fusion (reviewed in references 3 and 10). The R18 assay has been used successfully for monitoring the cell fusion mediated by the influenza virus HA when expressed in CV-1 cells from an SV40 vector (6). However, the assay could not be used successfully for the SV5 F proteins mutants described here. One explanation for this failure to obtain positive data from the assay is that the paramyxovirus F protein lacks the receptor-binding activity (hemagglutination) normally provided by the HN glycoprotein (and that is an inherent property of influenza virus HA) and thus there was no means of attaching the R18 loaded erythrocytes to the CV-1 cells expressing F.

The three SV5 F glycine mutants, G_3A, G_7A, and $G_{12}A$, all resulted in increased syncytium-inducing activity. Although both alanine and glycine are small neutral, aliphatic amino acids, this change in mutants G_7A and $G_{12}A$ had a drastic effect on the transport and maturation of the F protein as well as the fusion activity. Not only was the fusion activity of the glycine mutants increased, but the low level of cleavage and cell surface expression of these F mutants suggests that the specific activity of these molecules is greatly increased. The simplest interpretation of these data is that the F peptide is directly involved in syncytium formation. A two- to threefold increase in fusion activity of the SIV gp32 has been found when alanine was substituted for glycine, and it was suggested that the introduction of alanine increased the hydrophobicity of the F peptide, stabilizing its lipid interaction (4). As the SV5 F protein mutants $A_{10}V$ and $V_{13}I$ do cause an increase in hydrophobicity as measured by most criteria but do not exhibit increased fusogenic activity over wt F, these factors suggest that fusion activity involves more than increased hydrophobicity.

Although an X-ray structural determination of the paramyxovirus F protein has yet to be made, several studies suggest the fusion peptide forms an α-helix. The circular dichroism spectrum of the detergent-solubilized Sendai virus F protein indicated a greater α-helical component in the cleaved form than in the uncleaved form, concomitant with an increase in hydrophobicity of the protein (20). Additionally, synthetic peptides corresponding to the F_1 N-terminal domain of Newcastle disease virus increased their helicity and assumed an oblique transmembrane orientation when interacting with lipids (5). This orientation is also inferred for the SIV gp32 N terminus as mutations which, in theory, modify the potential to form an obliquely oriented α-helix caused a reduced fusion potential (17). For the influenza virus HA, a direct demonstration of the HA_2 N terminus interacting with the lipid bilayer was provided by transfer of label from a photoactive hydrophobic probe to the HA_2 N terminus, and the labeling pattern suggested that the domain was inserted into the membrane as an α-helix (14). In conjunction with the glycine-to-alanine mutants described here, it is worth noting that in a study of the helical C peptide of RNase A, when internal alanine residues were converted to glycine residues the α-helix was substantially destabilized (59). The substitution of glycine to alanine was found to increase the thermostability of three naturally occurring proteins: the lambda repressor, a *Bacillus stearothermophilus* protease, and the bacteriophage T4 lysozyme (59 and references therein). Thus, the potential for the F fusion peptide to form an α-helical structure is likely to be lessened by the presence of the helix-destabilizing glycine residues.

Host cell DNA, RNA, and protein synthesis, as well as virus production, is shut down during SV5 infection of fusion-susceptible BHK21-F cells (15). Thus, it was not surprising to find that the extensive fusion activity of G_7A and $G_{12}A$ correlated not only with an inhibition of protein synthesis, but also with an inability to produce high-titer SV40 stocks (data not shown). Although the detailed effect on SV40 replication was not investigated, extensive syncytium formation was observed beginning 60 h posttransfection of the SV40 F DNA, and the virus stocks had to be harvested prior to the usual time of 7 days posttransfection. The severity of the G_7A and $G_{12}A$ cytopathic effect may provide an explanation in part for the conservation of the F protein fusion peptide amino acid sequence. The invariant amino acids in the fusion peptide may preserve a balance between high fusion activity and successful viral replication. Substitution of alanine for glycine in mutants G_3A, G_7A, and $G_{12}A$ might stabilize the formation of an α-helix, perhaps lowering some energetic barriers to bilayer fusion. However, naturally occurring G_3A, G_7A, and $G_{12}A$ mutations, as well as others which have similar fusion characteristics, may be selected against, as they would limit viral replication. While

many mutations in the F fusion peptide can be accommodated without loss of fusion activity in cultured cells, the conserved sequence may help to stabilize the overall molecular architecture of the F protein. It is interesting that all six naturally occurring alanine residues align on the same face of the helix (Fig. 1B) and substituting alanine for glycine may serve to extend the length of the helical face containing alanine residues. The position of these alanine residues may be an important factor in the conservation of the fusion peptide sequence in the paramyxovirus F proteins, and this remains to be determined.

ACKNOWLEDGMENTS

We thank Reay G. Paterson for providing the SV5 F clones and the peptide antiserum used in this study and for reading the manuscript, Rick E. Randall for the F1a monoclonal antibody, Robert C. MacDonald and Ruby I. MacDonald for assistance with quantitation of cell fusion, Margaret A. Shaughnessy for excellent technical assistance, and the members of the Lamb laboratory for helpful discussions.

This work was supported by Research Grant AI-23173 from the National Institute of Allergy and Infectious Diseases. C.M.H. received support from a National Institutes of Health Training Program in Cell and Molecular Biology, GM-08061. R.A.L. is an Investigator of the Howard Hughes Medical Institute.

REFERENCES

1. **Allen, J. P., G. Feher, T. O. Yeates, H. Komiya, and D. C. Rees.** 1987. Structure of the reaction center from *Rhodobacter sphaeroides* R-26: the protein subunits. Proc. Natl. Acad. Sci. USA **84:**6162–6166.
2. **Asano, K., and A. Asano.** 1985. Why is a specific amino acid sequence of F glycoprotein required for the membrane fusion reaction between envelope of HVJ (Sendai virus) and target cell membranes? Biochem. Int. **10:**115–122.
3. **Blumenthal, R.** 1987. Membrane fusion. Curr. Top. Membr. Transp. **29:**203–254.
4. **Bosch, M. L., P. L. Earl, K. Fargnoli, S. Picciafuoco, F. Giombini, F. Wong-Staal, and G. Franchini.** 1989. Identification of the fusion peptide of primate immunodeficiency viruses. Science **244:**694–697.
5. **Brasseur, R., P. Lorge, E. Goormaghtigh, J.-M. Ruysschaert, D. Espion, and A. Burny.** 1988. The mode of insertion of the paramyxovirus F1 N-terminus into lipid matrix, and initial step in host cell/virus fusion. Virus Genes **4:**325–332.
6. **Clague, M. J., C. Schoch, and R. Blumenthal.** 1991. The delay time for influenza hemagglutinin-induced membrane fusion depends on the hemagglutinin surface density. J. Virol. **65:**2402–2407.
7. **Deisenhofer, J., O. Epp, K. Miki, R. Huber, and H. Michel.** 1985. Structure of the protein subunits in the photosynthetic reaction center of *Rhodopseudomonas virdis* at 3 Å resolution. Nature (London) **318:**618–624.
8. **Doyle, C., M. G. Roth, J. Sambrook, and M.-J. Gething.** 1985. Mutations in the cytoplasmic domain of the influenza virus hemagglutinin affect different stages of intracellular transport. J. Cell Biol. **100:**704–714.
9. **Dreyfuss, G., Y. D. Choi, and S. A. Adam.** 1984. Characterization of heterogeneous nuclear RNA-protein complexes in vivo with monoclonal antibodies. Mol. Cell. Biol. **4:**1104–1114.
10. **Duzgenes, N., and Bentz, J.** 1988. Fluorescence assays for membrane fusion, p. 3–21. *In* L. M. Loew (ed.), Spectroscopic membrane probes. CRC Press, Boca Raton, Fla.
11. **Gallaher, W. R.** 1987. Detection of a fusion peptide sequence in the transmembrane protein of human immunodeficiency virus. Cell **50:**327–328.
12. **Gething, M.-J., R. W. Doms, D. York, and J. White.** 1986. Studies on the mechanism of membrane fusion: site-specific mutagenesis of the hemagglutinin of influenza virus. Cell **46:**939–950.
13. **Gething, M. J., J. White, and M. D. Waterfield.** 1978. Purification of the fusion protein of Sendai virus: analysis of the NH_2-terminal sequence generated during precursor activation. Proc. Natl. Acad. Sci. USA **75:**2737–2740.
14. **Harter, C., P. James, T. Bachi, G. Semenza, and J. Brunner.** 1989. Hydrophobic binding of the ectodomain of the influenza hemagglutinin to membranes occurs through the "fusion peptide." J. Biol. Chem. **264:**6459–6464.
15. **Holmes, K. V., and P. W. Choppin.** 1966. On the role of the response of the cell membrane in determining virus virulence. Contrasting effects of the parainfluenza virus SV5 in two cell types. J. Exp. Med. **124:**501–531.
16. **Homma, M., and M. Ohuchi.** 1973. Trypsin action on the growth of Sendai virus in tissue culture cells. J. Virol. **12:**1457–1465.
17. **Horth, M., B. Lambrecht, M. C. L. Khim, F. Bex, C. Thiriart, J.-M. Ruysschaert, A. Burny, and R. Brasseur.** 1991. Theoretical and functional analysis of the SIV fusion peptide. EMBO J. **10:**2747–2755.
18. **Horvath, C. M., M. A. Williams, and R. A. Lamb.** 1990. Eukaryotic coupled translation of tandem cistrons: identification of the influenza B virus BM2 polypeptide. EMBO J. **9:**2639–2647.
19. **Hsu, M.-C., and P. W. Choppin.** 1984. Analysis of Sendai virus mRNAs with cDNA clones of viral genes and sequences of biologically important regions of the fusion protein. Proc. Natl. Acad. Sci. USA **81:**7732–7736.
20. **Hsu, M.-C., A. Scheid, and P. W. Choppin.** 1981. Activation of the Sendai virus fusion protein (F) involves a conformational change with exposure of a new hydrophobic domain. J. Biol. Chem. **256:**3557–3563.
21. **Hsu, M.-C., A. Scheid, and P. W. Choppin.** 1987. Protease activation mutants of Sendai virus: sequence analysis of the mRNA of the fusion protein (F) gene and direct identification of the cleavage-activation site. Virology **156:**84–90.
22. **Kawano, M., H. Bando, S. Ohgimoto, K. Kondo, M. Tsurudome, M. Nishio, and Y. Ito.** 1990. Sequence of the fusion protein gene of human parainfluenza type 2 virus and its intergenic region: lack of small hydrophobic (SH) gene. Virology **178:**289–292.
23. **Kunkel, T. A.** 1985. Rapid and efficient site-specific mutagenesis without phenotypic selection. Proc. Natl. Acad. Sci. USA **82:**488–492.
24. **Lamb, R. A., and P. W. Choppin.** 1976. Synthesis of influenza proteins in infected cells: translation of viral polypeptides, including three P polypeptides, from RNA produced by primary transcription. Virology **74:**504–519.
25. **Lamb, R. A., P. R. Etkind, and P. W. Choppin.** 1978. Evidence for a ninth influenza viral polypeptide. Virology **91:**60–78.
26. **Levitt, M.** 1978. Conformational preferences of amino acids in globular proteins. Biochemistry **17:**4277–4285.
27. **McGinnes, L. W., and T. G. Morrison.** 1986. Nucleotide sequence of the gene encoding the Newcastle disease virus fusion protein and comparisons of paramyxovirus fusion protein sequences. Virus Res. **5:**343–356.
28. **Merson, J. R., R. A. Hull, M. K. Estes, and J. A. Kasel.** 1988. Molecular cloning and sequence determination of the fusion protein of human parainfluenza virus type I. Virology **167:**97–105.
29. **Merz, D. C., A. Scheid, and P. W. Choppin.** 1980. Importance of antibodies to the fusion glycoprotein of paramyxoviruses in the prevention of spread of infection. J. Exp. Med. **151:**275–288.
30. **Merz, D. C., A. Scheid, and P. W. Choppin.** 1981. Immunological studies of the functions of paramyxovirus glycoproteins. Virology **109:**94–105.
31. **Morrison, T. G., and A. Portner.** 1991. Structure, function, and intracellular processing of the glycoproteins of paramyxoviridae. p. 347–382. *In* D. W. Kingsbury (ed.), The paramyxoviruses. Plenum Press, New York.
32. **Morrison, T. G., L. Ward, and A. Semerjian.** 1985. Intracellular processing of the Newcastle disease virus fusion glycoprotein. J. Virol. **53:**851–857.
33. **Ng, D. T. W., R. E. Randall, and R. A. Lamb.** 1989. Intracellular maturation and transport of the SV5 type II glycoprotein hemagglutinin-neuraminidase: specific and transient association with GRP78-BiP in the endoplasmic reticulum and extensive

internalization from the cell surface. J. Cell Biol. **109**:3273–3289.
34. **Novick, S. L., and D. Hoekstra.** 1988. Membrane penetration of Sendai virus glycoproteins during the early stages of fusion with liposomes as determined by hydrophobic photoaffinity labelling. Proc. Natl. Acad. Sci. USA **85**:7433–7437.
35. **Parks, G. D., and R. A. Lamb.** 1990. Defective assembly and intracellular transport of mutant paramyxovirus hemagglutinin-neuraminidase proteins containing altered cytoplasmic domains. J. Virol. **64**:3605–3616.
36. **Paterson, R. G.** Unpublished observation.
37. **Paterson, R. G., T. J. R. Harris, and R. A. Lamb.** 1984. Fusion protein of the paramyxovirus simian virus 5: nucleotide sequence of mRNA predicts a highly hydrophobic glycoprotein. Proc. Natl. Acad. Sci. USA **81**:6706–6710.
38. **Paterson, R. G., S. W. Hiebert, and R. A. Lamb.** 1985. Expression at the cell surface of biologically active fusion and hemagglutinin/neuraminidase proteins of the paramyxovirus simian virus 5 from cloned cDNA. Proc. Natl. Acad. Sci. USA **82**:7520–7524.
39. **Paterson, R. G., and R. A. Lamb.** 1987. Ability of the hydrophobic fusion-related external domain of a paramyxovirus F protein to act as a membrane anchor. Cell **48**:441–452.
40. **Paterson, R. G., R. A. Lamb, B. Moss, and B. R. Murphy.** 1987. Comparison of the relative roles of the F and HN surface glycoproteins of the paramyxovirus simian virus 5 in inducing protective immunity. J. Virol. **61**:1972–1977.
41. **Paterson, R. G., M. A. Shaughnessy, and R. A. Lamb.** 1989. Analysis of the relationship between cleavability of a paramyxovirus fusion protein and length of the connecting peptide. J. Virol. **63**:1293–1301.
42. **Peluso, R. W., R. A. Lamb, and P. W. Choppin.** 1977. Polypeptide synthesis in simian virus 5-infected cells. J. Virol. **23**:177–187.
43. **Randall, R. E., D. F. Young, K. K. A. Goswami, and W. C. Russell.** 1987. Isolation and characterization of monoclonal antibodies to simian virus 5 and their use in revealing antigenic differences between human, canine, and simian isolates. J. Gen. Virol. **68**:2769–2780.
44. **Richardson, C., D. Hull, P. Greer, K. Hasel, A. Berkovich, G. Englund, W. Bellini, B. Rima, and R. Lazzarini.** 1986. The nucleotide sequence of the mRNA encoding the fusion protein of measles virus (Edmonston strain): a comparison of fusion proteins from several different paramyxoviruses. Virology **155**: 508–523.
45. **Richardson, C. D., and P. W. Choppin.** 1983. Oligopeptides that specifically inhibit membrane fusion by paramyxoviruses: studies on the site of action. Virology **131**:518–532.
46. **Richardson, C. D., A. Scheid, and P. W. Choppin.** 1980. Specific inhibition of paramyxovirus and myxovirus replication by oligopeptides with amino acid sequences similar to those at the N-termini of the F_1 or HA_2 viral polypeptides. Virology **105**: 205–222.
47. **Rose, J. K., and J. E. Bergmann.** 1983. Altered cytoplasmic domains affect intracellular transport of the vesicular stomatitis virus glycoprotein. Cell **34**:513–524.
48. **Rose, J. K., and R. W. Doms.** 1988. Regulation of export from the endoplasmic reticulum. Annu. Rev. Cell Biol. **4**:257–288.
49. **Roth, M., A. Lewit-Bentley, H. Michel, J. Deisenhofer, R. Huber, and D. Oesterhelt.** 1989. Detergent structure in crystals of a bacterial photosynthetic reaction centre. Nature (London) **340**:659–662.
50. **Sakaguchi, T., Y. Matsuda, R. Kiyokage, N. Kawahara, K. Kiyotani, N. Katunuma, Y. Nagai, and T. Yoshida.** 1991. Identification of endoprotease activity in the trans Golgi membranes of rat liver cells that specifically processes in vitro the fusion glycoprotein precursor of virulent Newcastle disease virus. Virology **184**:504–512.
51. **Sanger, F., S. Nicklen, and A. R. Coulson.** 1977. DNA sequencing with chain-terminating inhibitors. Proc. Natl. Acad. Sci. USA **74**:5463–5467.
52. **Scheid, A., and P. W. Choppin.** 1974. Identification of biological activities of paramyxovirus glycoproteins. Activation of cell fusion, hemolysis, and infectivity by proteolytic cleavage of inactive precursor protein of Sendai virus. Virology **57**:475–490.
53. **Scheid, A., and P. W. Choppin.** 1977. Two disulfide-linked polypeptide chains constitute the active F protein of paramyxoviruses. Virology **80**:54–66.
54. **Scheid, A., M. Graves, S. Silver, and P. W. Choppin.** 1978. Studies on the structure and function of paramyxovirus glycoproteins, p. 181–193. *In* B. W. J. Mahy and R. D. Barry (ed.), Negative strand viruses and the host cell. Academic Press, London.
55. **Server, A. C., J. A. Smith, M. N. Waxham, J. S. Wolinsky, and H. M. Goodman.** 1985. Purification and amino terminal protein sequence analysis of the mumps virus fusion protein. Virology **144**:373–383.
56. **Sheshberaderan, H., and R. A. Lamb.** 1991. Simian virus 5 membrane protein maturation: expression in virus-infected cells and from a eukaryotic vector. Virology **183**:803–809.
57. **Spriggs, M. K., R. A. Olmstead, S. Venkatesan, J. E. Coligan, and P. L. Collins.** 1986. Fusion glycoprotein of human parainfluenza virus type 3: nucleotide sequence of the gene, direct identification of the cleavage-activation site, and comparison with other paramyxoviruses. Virology **152**:241–251.
58. **Stegmann, T., R. W. Doms, and A. Helenius.** 1989. Protein-mediated membrane fusion. Annu. Rev. Biophys. Biophys. Chem. **18**:187–211.
59. **Strehlow, K. G., and R. L. Baldwin.** 1989. Effect of the substitution Ala>Gly at each of five residue positions in the C-peptide helix. Biochemistry **28**:2130–2133.
60. **Toyoda, T., T. Sakaguchi, K. Imai, N. M. Inocencio, B. Gotoh, M. Hamaguchi, and Y. Nagai.** 1987. Structural comparison of the cleavage-activation site of the fusion glycoprotein between virulent and avirulent strains of Newcastle disease virus. Virology **158**:242–247.
61. **Tsukiyama, K., Y. Yoshikawa, and K. Yamanouchi.** 1988. Fusion glycoprotein (F) of rinderpest virus: entire nucleotide sequence of the F mRNA, and several features of the F protein. Virology **164**:523–530.
62. **Tsurodome, M., H. Bando, M. Nishio, Y. Iwamoto, M. Kawano, K. Kondo, H. Komada, and Y. Ito.** 1990. Antigenic and structural properties of a paramyxovirus simian virus 41 (SV41) reveal a close relationship with human parainfluenza type 2 virus. Virology **179**:738–748.
63. **Varsanyi, T. M., H. Jornvall, C. Orvell, and E. Norrby.** 1987. F_1 polypeptides of two canine distemper strains: variation in the conserved N-terminal hydrophobic region. Virology **157**:241–244.
64. **Von Heijne, G.** 1981. The amino acid composition of membrane-spanning segments. Eur. J. Biochem. **120**:275–278.
65. **Waxham, M. N., A. C. Server, H. M. Goodman, and J. S. Wolinsky.** 1987. Cloning and sequencing of the mumps virus fusion protein gene. Virology **159**:381–388.
66. **White, J., M. Kielian, and A. Helenius.** 1983. Membrane fusion proteins of enveloped animal viruses. Q. Rev. Biophys. **16**:151–195.
67. **White, J. M.** 1990. Viral and cellular fusion proteins. Annu. Rev. Physiol. **52**:675–697.
68. **Zebedee, S. L., and R. A. Lamb.** 1988. Influenza virus M_2 protein: monoclonal antibody restriction of virus growth and detection of M_2 in virions. J. Virol. **62**:2762–2772.